

Crystallization and preliminary X-ray analysis of *Weissella viridescens* FemX UDP-MurNAc-pentapeptide:L-alanine ligase

Sabrina Biarrotte-Sorin,^{a†}
Antoine P. Maillard,^{b†} Jean
Delettré,^a Wladimir Sougakoff,^c
Didier Blanot,^d Karine
Blondeau,^e Jean-Emmanuel
Hugonnet,^b Claudine Mayer^{a*}
and Michel Arthur^b

^aLaboratoire de Minéralogie-Cristallographie de Paris, Université Paris 6, Paris, France,

^bLaboratoire de Recherche Moléculaire sur les Antibiotiques, UFR Broussais-Hotel Dieu, Paris, France,

^cLaboratoire de Recherche Moléculaire sur les Antibiotiques, UFR Pitié-Salpêtrière, France,

^dEnveloppes Bactériennes et Antibiotiques, Université Paris Sud, Orsay, France,

and ^eInstitut de Génétique et de Microbiologie, Université Paris Sud, Orsay, France

† These authors contributed equally to the work.

Correspondence e-mail: mayer@lmcp.jussieu.fr

Synthesis of the cell-wall peptidoglycan of firmicutes involves a unique family of peptide-bond-forming enzymes that use amino-acyl-tRNAs as substrates and are referred to as Fem proteins as they are factors essential for methicillin resistance in *Staphylococcus aureus*. The FemX UDP-MurNAc-pentapeptide:L-alanine ligase of *Weissella viridescens* was overexpressed, purified and crystallized. Native data were collected to 1.7 Å resolution. The crystals belong to space group $P2_1$, with unit-cell parameters $a = 42.03$, $b = 99.92$, $c = 45.84$ Å, $\beta = 116.02^\circ$. The asymmetric unit contains one molecule. A selenium-derivative data set has been collected to 2.1 Å resolution at the peak wavelength of the selenium absorption edge. Six strong selenium positions were visible in the anomalous Patterson map. Three additional weaker Se atoms have been identified by anomalous Fourier synthesis.

Received 25 November 2002

Accepted 24 March 2003

1. Introduction

The bacterial cell-wall peptidoglycan is a network composed of glycan strands cross-linked by oligopeptides of variable composition and complexity (Schleifer & Kandler, 1972). Many species of firmicutes (formerly referred to as Gram-positive bacteria) produce branched peptidoglycan precursors resulting from the addition of a side chain to the ϵ -amino group of L-Lys in the pentapeptide stem L-Ala- γ -D-Glu-L-Lys-D-Ala-D-Ala (Schleifer & Kandler, 1972). Such side chains consist of five glycylic residues in *Staphylococcus aureus* (Rohrer *et al.*, 1999), two L-alanyl residues in *Enterococcus faecalis* (Bouhss *et al.*, 2001) and the sequence L-Ala-L-Ser in *Weissella viridescens* (Hegde & Shrader, 2001). Addition of these amino acids is catalyzed by a unique family of peptide-bond-forming enzymes that use amino-acyl-tRNAs as substrates (for a review, see Rohrer & Berger-Bächi, 2003). These enzymes are potential targets for the development of new antimicrobial agents as the side chain is used by the essential D,D-transpeptidases in the final cross-linking step of peptidoglycan synthesis (Bouhss *et al.*, 2002).

Benson *et al.* (2002) have recently solved the atomic structure of the FemA protein, which adds glycylic residues at the second and third positions of the *S. aureus* pentaglycine side chain. The structure reveals the presence of an antiparallel coiled-coil domain which has been proposed to be implicated in tRNA binding. However, sequence analyses show that this domain is not present in several members of

the Fem family, including FemX from *W. viridescens*. Unlike FemA, FemX has been demonstrated to add the first alanyl residue of the side chain of peptidoglycan precursors using alanyl-tRNA as a substrate (Plapp & Strominger, 1970). Here, we report the purification and crystallization of the *W. viridescens* FemX enzyme together with preliminary X-ray data analysis.

2. Method and results

2.1. Protein preparation

The *femX* gene of *W. viridescens* was cloned into the pTYB2 vector (New England Biolabs) and production of FemX fused to the C-terminal intein affinity tag (IMPACT-CN System, New England Biolabs) was induced in *Escherichia coli* ER2566 overnight at 289 K with isopropyl- β -D-thiogalactoside (0.3 mM). Incorporation of selenomethionine was obtained by inhibiting the methionine pathway as described by van Duyne *et al.* (1993). The fusion protein bound to chitin beads was cleaved overnight at 277 K with 50 mM β -mercaptoethanol, leaving an additional C-terminal glycylic residue in comparison to the wild-type gene product. The FemX monomer was further purified by anion-exchange and size-exclusion chromatography. Elution from the size-exclusion column (Superdex 75 HR10/30, Amersham Biosciences) provided a protein peak with an estimated mass of 42 kDa corresponding to the FemX monomer (retention volume of 10.65 ml with 25 mM Tris-HCl pH 7.5, 0.3 M NaCl, 2 mM β -mercaptoethanol as

the eluent). Amino-terminal sequencing showed loss of the N-terminal methionine. MALDI-TOF mass-spectrometry analyses provided peaks with m/z at 38 200 and 38 774 for native and selenomethionine-labelled FemX, in agreement with the molecular weights of 38 210 Da and 38 773 Da deduced from the FemX sequence (12 methionyl or selenomethionyl residues, respectively). Determination of the amino-acid composition after acid hydrolysis [6 M HCl containing 1:2000(v:v) β -mercaptoethanol, 378 K, 24 h] confirmed this result: methionine was not detected in the selenomethionine-labelled preparation of FemX (<0.3 residue per monomer).

2.2. Crystallization

We attempted initial screening of the crystallization conditions using Hampton Research Crystal Screens and the Stura Footprint Screen (Stura *et al.*, 1992) from Molecular Dimensions Ltd using the hanging-drop vapour-diffusion method at 295 K. The droplet size was 2 μ l, comprising equal volumes of protein and reservoir solution. Thin needle-like crystals were observed at 291 K in the Hampton Research Crystal Screen with 30% polyethylene glycol

8K as precipitant, 300 mM sodium chloride, 100 mM cacodylate pH 6.5 and 200 mM sodium acetate trihydrate. Improvement of the crystallization condition was essential in order to produce larger single crystals as they characteristically formed fragile and compact clusters (Fig. 1a). Additional screening experiments were made by variation of the concentration and the molecular weight of the PEG. Crystals grew to more than 1 mm in length but less than 50 μ m in cross-section. The best native crystals (Fig. 1b), which were suitable for high-resolution diffraction studies, were grown in 30% polyethylene glycol 6K, 300 mM sodium chloride and 100 mM cacodylate pH 6.5 to maximum size in 3 d (1 \times 0.02 \times 0.05 mm). The selenomethionine-labelled protein was crystallized under similar conditions using 25% polyethylene glycol 10K as precipitant with additional 400 mM sodium acetate and had an identical needle-like morphology.

2.3. Data collection and X-ray analysis

The crystals were mounted in a cryoloop and flash-frozen directly from the drop in the presence of 30% glycerol. Both diffraction data from the native and the SeMet protein were collected using a MAR CCD detector at beamline FIP-BM30A of the European Synchrotron Radiation Facility, Grenoble (Roth *et al.*, 2002). In many examples (Qian *et al.*, 2000; Yaremchuk *et al.*, 2000; Maté *et al.*, 1999), thin needle-like crystals are not of suitable quality for diffraction experiments. In the case reported here, the needle-shaped crystals diffract to higher than 1.7 Å and a complete native data set could

Table 1

Data-collection statistics for native and anomalous data sets.

Values in parentheses are for the highest resolution shell.

	Native	SeMet (peak)
X-ray source	FIP-BM30	FIP-BM30
Space group	$P2_1$	$P2_1$
Unit-cell parameters (Å , $^\circ$)	$a = 42.03$, $b = 99.92$, $c = 45.84$, $\beta = 116.02$	$a = 42.26$, $b = 101.32$, $c = 46.62$, $\beta = 115.55$
Data-collection statistics		
Wavelength (Å)	0.97976	0.98064
Resolution range (Å)	35.0–1.7	39.0–2.1
No. observations	156408	154237
No. unique reflections	36921	20691
Completeness (%)	98.8 (97.7)	99.9 (99.9)
Redundancy	4.2 (3.7)	7.5 (7.5)
R_{sym}^\dagger (%)	4.4 (13.9)	8.6 (12.3)‡
$I/\sigma(I)$	10.2 (3.7)	6.5 (10.1)§
		7.5 (6.2)

$^\dagger R_{\text{sym}} = \sum |I - \langle I \rangle| / \sum I$, where I is the intensity of an individual reflection and $\langle I \rangle$ is its mean value. ‡ Bijvoets pairs were merged. § Bijvoets pairs were not merged.

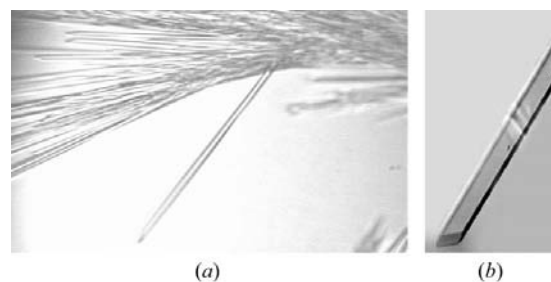


Figure 1
(a) Typical cluster of needle-like FemX crystals. (b) Typical crystal of FemX with dimensions of 1.0 \times 0.05 \times 0.02 mm.

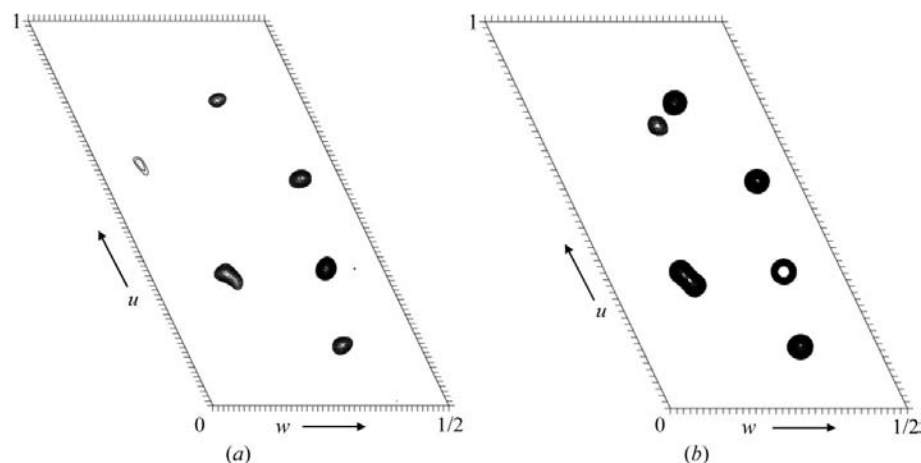


Figure 2
 $v = 0.5$ section of (a) the experimental and (b) the predicted anomalous Patterson map calculated at 15.0–2.1 Å resolution.

be collected to 1.7 Å resolution with a 210° sweep. Data were processed using *MOSFLM* (Powell, 1999) and *SCALA* from the *CCP4* program suite (Collaborative Computational Project, Number 4, 1994). Autoindexing and consideration of systematically absent reflections revealed that the crystals belong to the monoclinic space group $P2_1$, with one molecule in the asymmetric unit ($V_M = 2.2 \text{ Å}^3 \text{ Da}^{-1}$) and 44% solvent content. Attempts to solve the structure by molecular replacement using the FemA structure (Benson *et al.*, 2002) without the coiled-coil domain failed. As crystals could be obtained from the selenium derivative, an SeMet SAD data set was collected at the selenium peak wavelength (0.98064 Å) with a 360° sweep. The selenium-derivative crystals diffract to 2.1 Å resolution. The data-collection statistics are summarized in Table 1. Six selenium sites were clearly visible in the anomalous Patterson synthesis map calculated between 15 and 2.1 Å resolution with the program *CNS* (Brünger *et al.*, 1998; Fig. 2). The combination of an anomalous difference map and a gradient map allowed the location of three additional Se atoms. Heavy-atom refinement and phasing to 2.1 Å , which were performed using *CNS*, resulted in phases with a figure of merit of 0.406 and a phasing power of 1.70. After density modification, the map was clearly interpretable and was submitted to the automatic *wARP* procedure (Perrakis *et al.*, 1999). The structure has been refined and will be published elsewhere; coordinates have been deposited in the Protein Data Bank under accession code 1ne9.

We thank Dr Jean-Luc Ferrer and Dr Michel Pirrochi from the FIP-BM30A beamline at the ESRF for assistance with data collection and Olivier Poch for helpful support in sequence analyses. This work was supported by the Ministère de la Recherche (grant ACI252 'Molécules et cibles thérapeutiques'), the Programme de Recherche Fondamentale en Microbiologie et Maladies Infectieuses et Parasitaires (MENRT) and by the Fondation pour la Recherche Médicale.

References

- Benson, T., Prince, D., Mutchler, V., Curry, K., Ho, A., Sarver, R., Hagadorn, J., Choi, G. & Garlick, R. (2002). *Structure*, **10**, 1107–1115.
- Bouhss, A., Josseaume, N., Allanic, D., Crouvoisier, M., Gutmann, L., Mainardi, J.-L., Mengin-Lecreulx, D., van Heijenoort, J. & Arthur, M. (2001). *J. Bacteriol.* **183**, 5122–5127.
- Bouhss, A., Josseaume, N., Severin, A., Tabei, K., Hugonnet, J. E., Shlaes, D., Mengin-Lecreulx, D., Van Heijenoort, J. & Arthur, M. (2002). *J. Biol. Chem.* **277**, 45935–45941.
- Brünger, A. T., Adams, P. D., Clore, G. M., DeLano, W. L., Gros, P., Grosse-Kunstleve, R. W., Jiang, J.-S., Kuszewski, J., Nilges, M., Pannu, N. S., Read, R. J., Rice, L. M., Simonson, T. & Warren, G. L. (1998). *Acta Cryst.* **D54**, 905–921.
- Collaborative Computational Project, Number 4 (1994). *Acta Cryst.* **D50**, 760–763.
- Hegde, S. S. & Shrader, T. E. (2001). *J. Biol. Chem.* **276**, 6998–7003.
- Maté, M. J., Ortiz-Lombardía, M., Marina, A. & Fita, I. (1999). *Acta Cryst.* **D55**, 1066–1068.
- Perrakis, A., Morris, R. & Lamzin, V. S. (1999). *Nature Struct. Biol.* **6**, 458–463.
- Plapp, R. & Strominger, J. L. (1970). *J. Biol. Chem.* **245**, 3675–3682.
- Powell, H. (1999). *Acta Cryst.* **D55**, 1690–1695.
- Qian, C., Lagacé, L., Massariol, M.-J., Chabot, C., Yoakim, C., Déziel, R. & Tong, L. (2000). *Acta Cryst.* **D56**, 175–180.
- Rohrer, S. & Berger-Bächi, B. (2003). *Antimicrob. Agents Chemother.* **47**, 837–846.
- Rohrer, S., Ehlert, K., Tschierske, M., Labischinski, H. & Berger-Bächi, B. (1999). *Proc. Natl. Acad. Sci. USA*, **96**, 9351–9356.
- Roth, M., Carpentier, P., Kaikati, O., Joly, J., Charraut, P., Pirocchi, M., Kahn, R., Fanchon, E., Jacquamet, L., Borel, F., Bertoni, A., Israel-Gouy, P. & Ferrer, J.-L. (2002). *Acta Cryst.* **D58**, 805–814.
- Schleifer, K. H. & Kandler, O. (1972). *Bacteriol. Rev.* **36**, 407–477.
- Stura, E. A., Nemerow, G. R. & Wilson, I. A. (1992). *J. Cryst. Growth*, **122**, 273–285.
- Van Duyne, G. D., Standaert, R. F., Karplus, P. A., Schreiber, S. L. & Clardy, J. (1993). *J. Mol. Biol.* **229**, 105–124.
- Yaremchuk, A., Cusack, S., Gudzera, O., Grötli, M. & Tukalo, M. (2000). *Acta Cryst.* **D56**, 667–669.